



All-optical nanopositioning of high-Q silica microspheres

RAFINO M. J. MURPHY, FUCHUAN LEI,* JONATHAN M. WARD, YONG YANG, AND SÍLE NIC CHORMAIC

Light-Matter Interactions Unit, Okinawa Institute of Science and Technology Graduate University, Onna, Okinawa 904-0495, Japan

**fuchuan.lei@oist.jp*

Abstract: A tunable, all-optical, coupling method is realised for a high- Q silica microsphere and an optical waveguide. By means of a novel optical nanopositioning method, induced thermal expansion of an asymmetric microsphere stem for laser powers up to 211 mW is observed and used to fine tune the microsphere-waveguide coupling. Microcavity displacements ranging from $(0.61 \pm 0.13) - (3.49 \pm 0.13) \mu\text{m}$ and nanometer scale sensitivities varying from $(2.81 \pm 0.08) - (17.08 \pm 0.76) \text{ nm/mW}$, with an apparent linear dependency of coupling distance on stem laser heating, are obtained. Using this method, the coupling is altered such that the different coupling regimes are achieved.

© 2017 Optical Society of America

OCIS codes: (070.5753) Resonators; (140.3948) Microcavity devices.

References and links

1. Y. Zhi, X.-C. Yu, Q. Gong, L. Yang, and Y.-F. Xiao, "Single nanoparticle detection using optical microcavities," *Adv. Mater.* **29**, 1604920 (2017).
2. G. C. Righini and S. Soria, "Biosensing by WGM microspherical resonators," *Sensors (Switzerland)* **16**, 1–25 (2016).
3. J. M. Ward, N. Dhasmana, and S. Nic Chormaic, "Hollow core, whispering gallery resonator sensors," *Eur. Phys. J. Spec. Top* **223**, 1917–1935 (2014).
4. Y. Yang, S. Saurabh, J. M. Ward, and S. Nic Chormaic, "High- Q , ultrathin-walled microbubble resonator for aerostatic pressure sensing," *Opt. Express* **24**, 294–299 (2016).
5. A. Matsko, *Practical Applications of Microresonators in Optics and Photonics* (CRC Press, 2009), 1st ed.
6. T. Aoki, B. Dayan, E. Wilcut, W. P. Bowen, A. S. Parkins, T. Kippenberg, K. Vahala, and H. Kimble, "Observation of strong coupling between one atom and a monolithic microwire resonator," *Nature* **443**, 671–674 (2006).
7. Y. Yang, F. Lei, S. Kasumie, L. Xu, J. M. Ward, L. Yang, and S. Nic Chormaic, "Tunable erbium-doped microbubble laser fabricated by sol-gel coating," *Opt. Express* **25**, 1308–1313 (2017).
8. J. M. Ward, Y. Yang, and S. Nic Chormaic, "Glass-on-glass fabrication of bottle-shaped tunable microlasers and their applications," *Sci. Rep.* **6**, 25152 (2016).
9. F.-C. Lei, M. Gao, C. Du, Q.-L. Jing, and G.-L. Long, "Three-pathway electromagnetically induced transparency in coupled-cavity optomechanical system," *Opt. Express* **23**, 11508–11517 (2015).
10. Y. Yang, X. Jiang, S. Kasumie, G. Zhao, L. Xu, J. M. Ward, L. Yang, and S. Nic Chormaic, "Four-wave mixing parametric oscillation and frequency comb generation at visible wavelengths in a silica microbubble resonator," *Opt. Lett.* **41**, 5266–5269 (2016).
11. Q.-T. Cao, H. Wang, C.-H. Dong, H. Jing, R.-S. Liu, X. Chen, L. Ge, Q. Gong, and Y.-F. Xiao, "Experimental demonstration of spontaneous chirality in a nonlinear microresonator," *Phys. Rev. Lett.* **118**, 033901 (2017).
12. M. Sumetsky, Y. Dulashko, and R. S. Windeler, "Optical microbubble resonator," *Opt. Lett.* **35**, 898–900 (2010).
13. K. Tada, G. Cohoon, K. Kieu, M. Mansuripur, and R. Norwood, "Fabrication of high- Q microresonators using femtosecond laser micromachining," *IEEE Photon. Techn. Lett.* **25**, 430–433 (2013).
14. S. Maayani, L. L. Martin, and T. Carmon, "Water-walled microfluidics for high-optical finesse cavities," *Nature Comm.* **7**, 10435 (2016).
15. X.-F. Liu, F. Lei, M. Gao, X. Yang, G.-Q. Qin, and G.-L. Long, "Fabrication of a microtoroidal resonator with picometer precise resonant wavelength," *Opt. Lett.* **41**, 3603–3606 (2016).
16. X. Xu, X. Jiang, G. Zhao, and L. Yang, "Phone-sized whispering-gallery microresonator sensing system," *Opt. Express* **24**, 25905–25910 (2016).
17. J. C. Knight, G. Cheung, F. Jacques, and T. A. Birks, "Phase-matched excitation of whispering-gallery-mode resonances by a fiber taper," *Opt. Lett.* **22**, 1129–1131 (1997).
18. M. Cai, O. Painter, and K. J. Vahala, "Observation of critical coupling in a fiber taper to a silica-microsphere whispering-gallery mode system," *Phys. Rev. Lett.* **85**, 74–77 (2000).

19. J.P. Laine, C. Tapalian, B. Little, H.A. Haus, Acceleration sensor based on high-Q optical microsphere resonator and pedestal antiresonant reflecting waveguide coupler, *Sensors and Actuators A* **93**, 1-7. (2001).
20. X. Yang, S.K. Özdemir, B. Peng, H. Yilmaz, F.-C. Lei, G.-L. Long, and L. Yang, "Raman gain induced mode evolution and on-demand coupling control in whispering-gallery-mode microcavities," *Opt. Express* **23**, 29573–29583 (2015).
21. C. Yang, X. Jiang, Q. Hua, S. Hua, Y. Chen, J. Ma, and M. Xiao, "Realization of controllable photonic molecule based on three ultrahigh-Q microtoroid cavities," *Laser Photon. Rev.* **11**, 1600178 (2017).
22. S. G. Demos, R. A. Negres, R. N. Raman, A. M. Rubenchik, and M. D. Feit, "Material response during nanosecond laser induced breakdown inside of the exit surface of fused silica," *Laser Photon. Rev.* **7**, 444–452 (2013).
23. N. Bloembergen, "Role of cracks, pores, and absorbing inclusions on laser induced damage threshold at surfaces of transparent dielectrics," *Appl. Opt.* **12**, 661–664 (1973).

1. Introduction

Whispering gallery mode (WGM) resonators have shown much promise in terms of their versatility and scope in the last number of decades. These microcavities, with inherently small mode volumes (V_m) and high- Q factors, allow for strong light-matter interactions and have become widely used in bio-sensing and nanoparticle detection [1, 2], temperature, refractive index and pressure sensing [3,4] quantum optics and electrodynamics [5,6], microlaser development [7,8], and as a means of exploring optomechanical [9] and nonlinear effects [10,11]. Despite extensive research on microcavities of various geometries, fabrication methods, and properties [12–15], the commonplace bulky experimental apparatus used in microresonator experiments has impeded their successful incorporation into many lab-on-a-chip or miniaturized systems [16].

When conducting experiments of this nature, it is imperative that the coupling between the microresonator and waveguide can be manipulated in such a way that a high coupling efficiency and low loss are maintained. It was first noted by Knight et al. [17] that a tapered silica fiber could be used to excite high- Q whispering gallery modes in silica microspheres. Later, Cai et al. [18] observed a critical coupling regime for the same experimental framework. The ease with which tapered fibers can be integrated into optical networks, as well as their inherent high coupling efficiency, are some of the many characteristics that make tapered fibers a favored option over other coupling methods (e.g. a prism).

In order to further augment the sensitivity of these WGM systems post-fabrication, the coupling between a given resonator and optical source must be ameliorated. With regards to microsphere resonator systems, finely tuned coupling is usually achieved by means of a mechanical or piezoelectric nanometer resolution positioner. Albeit useful, such devices are difficult to incorporate into miniaturized microsphere or lab-on-a-chip systems that require a tunable coupling mechanism [19]. Other non-mechanical means of realizing coupling regime control have been explored in the past [20]. In this paper, we examine a means of achieving nanometer scale tunable coupling by taking advantage of thermo-mechanical effects arising from asymmetric microsphere stem fabrication, external laser heating, and thermal expansion in single mode optical fiber.

In principle, the scope of this work does not have to be restricted to microresonator coupled waveguide frameworks. With careful development and implementation this method could be used within photonic molecule systems as a means of varying the coupling between adjacent microcavities [21] and enhancing light-matter interactions, or perhaps as a micron scale nanostage, where the sphere acts as a holder for objects which can then be positioned by simply varying the laser power.

2. Fabrication method

Silica microspheres were made in the standard manner using a focused CO₂ beam (total power ~25 W) directed onto a piece of silica single-mode optical fiber (Thorlabs SMF-28). A small weight attached to the bottom of the fiber upon heating ensured the formation of a tapered sec-

tion which acts as the stem of the microsphere. By using a beam that was focused to a spot size smaller than the fiber diameter and adjusting the position of the CO₂ beam such that the heating was predominantly on one side of the fiber, an asymmetry was formed during tapering. If the core is too straight, light will pass from the stem to the end of the microsphere, resulting in no scattering within the stem, no thermo-mechanical effects and no microsphere displacement. In some samples we attempted to induce further asymmetry by reducing the spot size as much as possible and then pulsing the laser power in order to mimic an etching-like process via ablation – essentially carving the asymmetry out of the fiber. The deformation resulting from tapering and/or additional ablation caused the fiber core to taper towards one side, thus directing any incident light towards the asymmetric region (see Fig. 1(e)). The next stage of the fabrication process involved defocussing the laser beam and heating the optical fiber away from the stem. The melted silica at the fiber tip assumed a spherical morphology, due to surface tension. Finally, we conducted further broad-focus laser heating of the microsphere to reduce surface irregularities. Naturally, as the crux of the device is the skewed fiber core, it was at times difficult to control precisely. By slightly varying the fabrication method, the asymmetric stem/skewed fiber core was achieved. However, once a method was found we could consistently produce samples that exhibited this behavior. Post fabrication, the opposite end of the microsphere fiber was spliced to the output from a 980 nm laser diode, which was a standard EDFA pump type laser with a linewidth of a few nanometers and a maximum output power of 211 mW.

3. Asymmetry and heating effects

Normally, when light passes from the end of an optical fiber to the surrounding medium there are minimal thermal effects. The light traversing the dielectric material passes through a predominantly uniform cross-sectional area, a , into the surrounding medium with no heating of the silica. In our samples, the direction of propagation of light within the fiber appears to be directed towards their respective asymmetric stem regions (see Fig. 1). The behavior suggests that, for a given sample, the fiber core has been bent to one side; however, we cannot know this directly. Nevertheless, it is not unreasonable to assume that the core has been deformed during the fabrication process, or at the very least, the fiber has been warped in such a way that the 980 nm laser light is focused to one side. The geometry appears to prevent the laser light from passing unimpeded from the symmetric cylindrical region of the optical fiber to the end of the microsphere.

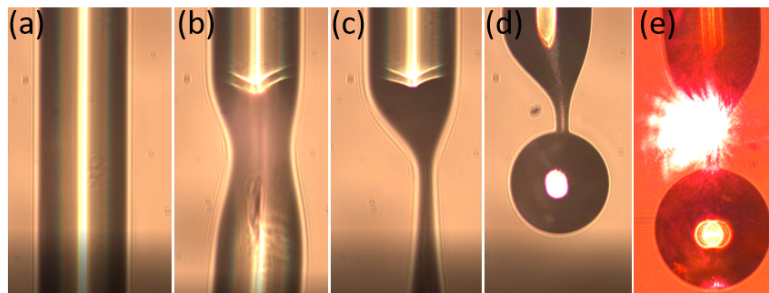


Fig. 1. Asymmetric stem fabrication. (a) - (c): The initial state of the optical fiber and the initial asymmetry resulting from side heating with a sub-fiber diameter CO₂ laser spot size and ~ 12% power. (d) - (e): Final asymmetric-stem microsphere sample after fabrication, highlighting the 980 nm laser scattering region. A video of the fabrication process is available (see [Visualization 1](#)).

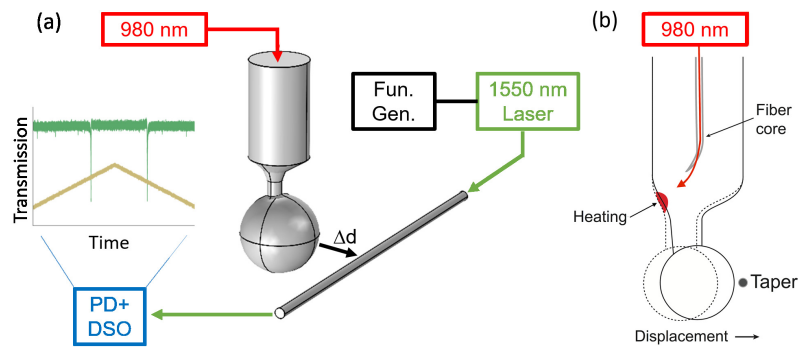


Fig. 2. (a) Schematic diagram of the experimental set-up used to characterize the tunable thermo-mechanical coupling. DSO: Digital Storage Oscilloscope; PD: Photodiode; FG: Function generator. (b) Deformation of the fiber during fabrication redirects the incident laser light towards the asymmetric stem. The local surface conditions of the asymmetric stem region, once exposed to the external 980 nm laser source, exhibit localized heating and thermal expansion of the silica (red: an example of a scattering/heating region), leading to an increase (or decrease) in the coupling distance, Δd . For the sake of clarity, Δd here is the distance between the microsphere and the tapered fiber.

The effects of laser energy deposition and laser damage on imperfect/deformed dielectric surfaces has been thoroughly examined over the last few decades [22, 23]. The aforementioned research suggests that these imperfections – such as nanometer to micrometer-scale cracks or spherical pores – can alter the amount of energy deposited at the laser-dielectric interaction boundary. The preceding experimental results have led us to conclude that the deformation of the fiber and geometry of the asymmetric stem invoke local surface conditions that induce scattering of the light within the stem, resulting in uneven energy deposition throughout the silica, localized heating, and thermal expansion. The net thermal expansion manifests as a linear displacement of the microsphere such that, when placed in a WGM coupling set-up, an increase or decrease in tapered fiber transmission is observed, depending on the orientation of the microsphere.

4. Tunable thermo-mechanical coupling characterization

In order to isolate the aforementioned microsphere displacement and ascertain how it affects coupling efficiency, we used a standard WGM resonator-tapered fiber set-up (see Fig. 2(a)). As a means of checking the validity of our hypothesis, the location of the scattering region was examined first, after which the microsphere was positioned such that the asymmetry was present in the plane perpendicular to the tapered fiber so that the sphere moved towards/away from the tapered fiber with increasing 980 nm laser power (see Fig. 2(b)). The orientation of the microsphere is important; if the displacement is not perpendicular to the fiber then the change in coupling is not maximized, or may not be observed at all. Using a piezoelectric nano-positioning stage (Thorlabs 3-Axis Piezo Controller MDT693A), the microsphere was brought close to the tapered fiber without initiating contact. Occasionally, the microsphere came into contact with the fiber directly while undergoing displacement. Out of the fabricated samples, none of them could be separated after contact by using the 980 nm laser. It is probable that the total microsphere displacement is small enough (and the fiber flexible enough) such that the tapered fiber remains in contact/bends with the sphere while it moves.

The coupling depth of the selected mode in the observed transmission spectrum and the piezo voltage (V_c) were used as initial position references. The laser power was then incremented from 0 to 211 mW, causing the coupling depth of the chosen mode in the transmission spectrum to change. Then, by means of the piezoelectric nano-positioning stage, the microsphere was moved

until the initial coupling depth was reinstated. The voltage difference applied to the piezo stage between this new position (V_o) and the initial reference position (V_c) was used to determine the change in coupling distance ($\Delta d = |V_c - V_o| \times k_p$), where the measured sensitivity (k_p) of the piezo stage was $0.36 \mu\text{m}/\text{V}$ and the rated resolution of the piezo stage was 36 nm . In order to exclude the possibility of cavity heating causing the observed transmission spectrum change, the relative change in transmission over the whole laser power range was determined for each sample. Also, as an extra means of precaution, each sample's non-contact transmission spectrum was obtained then isolated for a period of time. If the coupling did not vary over time, the subsequent results that were taken were deemed valid.

The change in coupling distance, Δd , for four independent samples, A, B, C and D is shown in Fig. 3. The results suggest a change in coupling distance with increasing laser power. By checking the orientation of the microsphere and examining the scattering region of the light in each case (see Fig. 1(e)), the results are consistent with the thermal deformation/stem thermal expansion hypothesis. Samples A, B, C and D exhibited displacement sensitivities of (4.42 ± 0.12) , (7.39 ± 0.17) , (2.81 ± 0.08) and $(17.08 \pm 0.76) \text{ nm}/\text{mW}$ and total displacements Δd of $0.61 \mu\text{m}$, $1.04 \mu\text{m}$, $1.58 \mu\text{m}$ and $3.49 \mu\text{m}$, respectively. Quantifying why one sample has larger displacement over another is difficult because the length starts at the position (and size) of the hot spot and this is not precisely known. Also the displacement depends on the length and the diameter of the stem which is not uniform. The transmission spectra for different input powers of the 980 nm laser, for sample D, can be seen in [Visualization 2](#).

Whether or not the thermal deformation of the stem could be used to traverse the different coupling regimes (under, critical and over-coupling) was also examined. For a particular mode, in sample D, the laser power was increased from $0 - 175 \text{ mW}$ while the transmission spectrum for each power increment was recorded. This sample was also examined while increasing and decreasing the 980 nm laser power in order to show the reversibility of the thermal deformation/expansion process. Examination of a particular mode with laser power variation over 175 mW shows evidence of traversing the different coupling regimes (see Fig. 4(a)). Un-

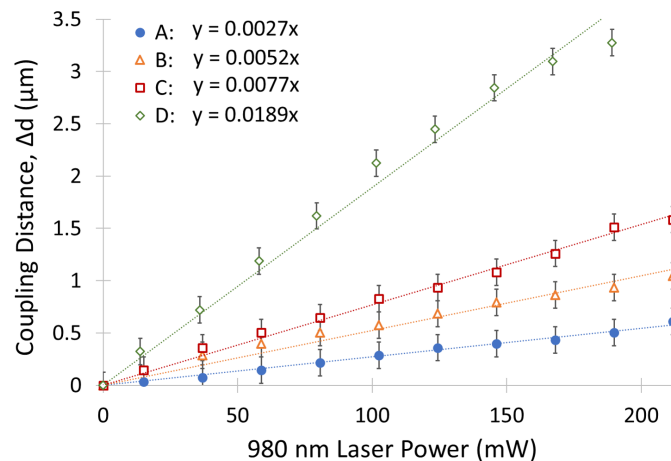


Fig. 3. Graph of coupling distance, Δd , against laser power for four samples A, B, C and D. The results indicate a linear increase in coupling distance with increasing laser power for these microsphere orientations, consistent with the thermal expansion hypothesis when the orientation and scattering regions are taken into consideration. Displacement sensitivities of (2.81 ± 0.08) , (4.42 ± 0.12) , (7.39 ± 0.17) and $(17.08 \pm 0.76) \text{ nm}/\text{mW}$ and a total Δd of (0.61 ± 0.13) , (1.04 ± 0.13) , (1.58 ± 0.13) , and $(3.49 \pm 0.13) \mu\text{m}$ are observed. Errors include the minimum resolution of the piezo stage of 36 nm as well as maximum observed fluctuation of the coupling depth for a given mode.

like in Fig. 3, the laser power was ramped from zero to maximum at a rate of 20 mHz. Initially, the microsphere was at a distance, Δd , such that the mode was strongly under-coupled with the on-resonance transmission at 93% (off-resonance transmission is defined as 100%). As the laser power was increased and Δd decreased, the coupling of the mode increased until the mode reached the critical coupling regime with on-resonance transmission of 1.4%. As the laser power reached a maximum and the coupling distance between the microsphere and tapered fiber decreased, the mode entered an over-coupled regime with the on-resonance transmission increasing to 96%. As the laser power decreased, the coupling followed the reverse trend with a bistable-like behavior, see Fig. 4(a). We believe this is due to the thermal response of the glass. To investigate this, the laser power was switched on and off and the mode coupling was recorded. When the laser was suddenly switched on/off it would take the modes approx. 1.5 sec. to reach a steady coupling condition (see Fig. 4(b)). When the laser power was increased in steps and steady state was achieved between each step, as in Fig. 3, the coupling behavior was symmetric for increasing and decreasing 980 nm laser powers. In some samples there was no noticeable red shifting of the WGMs due to heating by the 980 nm pump. However, in sample D some laser light was able to travel to the sphere and cause heating. For Fig. 4(a) the total red shift was 12 GHz.

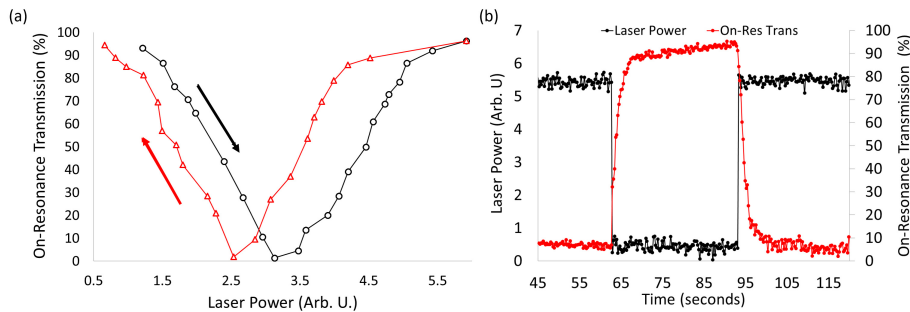


Fig. 4. (a) On-resonance transmission as a function of the 980 nm laser power for sample D. The Q -factor of the microsphere sample is $\sim 10^8$. (b) Change in coupling versus time when the 980 nm laser is switched on and off between 0 and 175 mW.

5. Conclusion

In conclusion, we have used an 980 nm laser and asymmetric-stem microsphere system to develop a tunable, thermo-mechanical coupling method within a WGM resonator-tapered fiber waveguide coupling system. Examination of this optical nanopositioning device with four independent samples shows a linear dependency of coupling distance with laser power, with sensitivities ranging from $(2.81 \pm 0.08) - (17.08 \pm 0.76)$ nm/mW. Under the right local conditions within the microsphere stem, traversing the different coupling regimes using this method was possible. In the future, this method could be used as a means of enabling tunable microsphere coupling in miniaturized or lab-on-a-chip resonator systems, photonic molecule systems and other nanopositioning systems.

Funding

Okinawa Institute of Science and Technology Graduate University.